analytical chemistry

pubs.acs.org/ac Article

BRET Q-Body: A Ratiometric Quench-based Bioluminescent Immunosensor Made of Luciferase−Dye−Antibody Fusion with Enhanced Response

Riho Takahashi, Takanobu Yasuda, Yuki Ohmuro-Matsuyama, and Hiroshi Ueda*

Cite This: *Anal. Chem.* 2021, 93, 7571−7578 Read Online

ACCESS | Metrics & More | Article Recommendations | Supporting Information

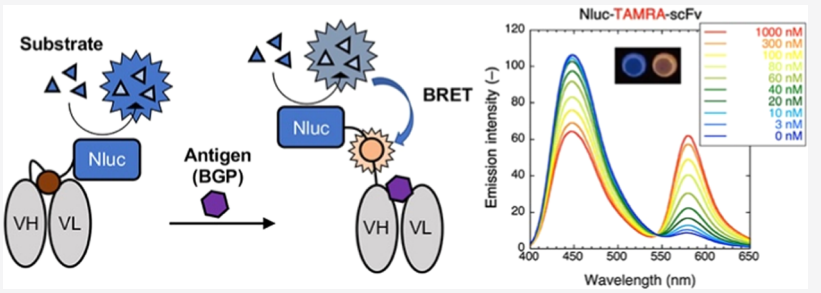

ABSTRACT: A quenchbody (Q-body) is an immunosensor comprising an antibody fragment containing an antigen-binding site that is site-specifically labeled with a fluorescent dye. The fluorescent dye of a Q-body is quenched in the absence of an antigen; however, its fluorescence recovers in the presence of an antigen, offering simple and rapid systems for antigen detection. In this study, we fused luciferase NanoLuc to a Q-body to construct a new immunosensor termed the "BRET Q-body" that can detect antigens based on the bioluminescence resonance energy transfer (BRET) principle. The resulting BRET Q-bodies for an osteocalcin peptide that emit three different emission colors could detect an antigen without the requirement of an external light source, based on ratiometric detection and color change with two wavelengths for the luciferase and fluorophore. Furthermore, the BRET Q-body produced unexpectedly higher responses up to 12-fold because of the increased BRET efficiency, probably associated with antigen-dependent dye movement. Thus, the BRET Q-body is a useful biosensor as a core of point-of-care tests.

Immunoassays represent an indispensable class of detection means in various fields, including biological research,[1−4] clinical diagnosis,[5−8] food safety management,[9−11] and environmental preservation.[12−14] Quenchbodies (Q-bodies) are antibody fragments containing an antigen-binding site and a site-specifically introduced fluorescent dye, and have been proven useful as immunosensors for a range of targets.[15−18] In the absence of an antigen, the fluorescent dye in a Q-body is quenched primarily by the photoinduced electron transfer from tryptophan (Trp) residues in the antibody variable region. When an antigen is added to the system, the fluorescent dye is released from the antibody molecule owing to antigen binding and no longer can contact Trp, recovering fluorescence (Figure 1A). Therefore, Q-bodies are expected to be applied for various analyses as immunoassay components capable of simple and rapid antigen detection by measuring only fluorescence intensity.[19−24] Meanwhile, previous Q-body-based antigen detection systems had some limitations. For example, an external light source is required for excitation of the dye and the absolute concentration of the Q-body must be known to quantify the antigen such as in intracellular assays because the fluorescence spectrum remains unchanged. Although ratiometric measurement was previously achieved by dual dye labeling, it needed a special labeling system using cell-free translation.

In this study, we aimed to fuse a bright luciferase, NanoLuc (Nluc),[25,26] to a Q-body to construct a highly sensitive immunosensor termed the "BRET Q-body" (Figure 1B) that can detect antigens based on the bioluminescence resonance energy transfer (BRET) principle.[27−32] Nluc is a luminescent enzyme derived from deep-sea shrimp *Oplophorus gracilirostris*, created by introducing 16 residue mutations into its catalytically active 19 kDa subunit. The luminescent substrate 2-furanylmethyl-deoxy-coelenterazine (furimazine) consumes oxygen and emits light in the reaction with Nluc. The luminescent substrate furimazine reacts with Nluc by consuming oxygen and emits light with a luminescence peak at around 460 nm. Its luminescence intensity is 80−240 times

Received: December 13, 2020
Accepted: May 6, 2021
Published: May 20, 2021

https://doi.org/10.1021/acs.analchem.0c05217
Anal. Chem. 2021, 93, 7571−7578

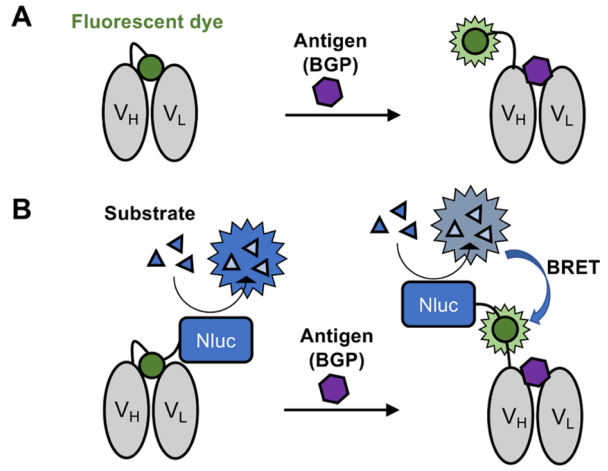

Figure 1. Scheme for working mechanisms of the Q-body (A) and the bioluminescence resonance energy transfer (BRET) Q-body (B). In (A), the fluorescence of the dye is quenched by the internal Trp residues of the antibody V region composed of the two variable region fragments V_H and V_L. Addition of the antigen results in the outward movement of the quenched dye, resulting in dequenching and fluorescence recovery. In (B), NanoLuc (Nluc) is fused to a Q-body to transfer luminescent energy to the dye, enabling ratiometric antigen quantitation without light irradiation.

higher than that of firefly luciferase, and its activity is maintained after incubation at 55 °C. Owing to its small size, it can be used for applications restricted to protein size. Such characteristics led to the use of Nluc in BRET assays, resulting in a new BRET methodology called NanoBRET.[27,33] Also, BRET-based immunosensors using Nluc as a reporter for detecting specific antibodies and antigens were reported.[34−36]

To investigate the possibility of combining the Nluc-based BRET assay and the Q-body technology, Nluc was fused to the N- or C-terminus of a single-chain antibody (scFv) fragment that specifically binds osteocalcin (bone Gla-protein, BGP), and the resulting fusion protein was labeled with a dye to prepare a BRET Q-body. Without the necessity of an external light source, the resulting BRET Q-body was predicted to permit ratiometric detection at two wavelengths for Nluc and the fluorescent dye. This is because the dye is quenched in the absence of the antigen and therefore Nluc glows when the luminescent substrate is used, while the dye is released from the antibody in the presence of the antigen and thus the emission produced from the dye is increased.

MATERIALS AND METHODS

Materials. The full sources of the materials used in this study are summarized in the "Materials and Methods" section in the Supporting Information (SI). The antigen peptides BGP-C7 (NH_2-RRFYGPV-COOH) and biotinylated BGP-C11 (Bio-QEAYRRFYGPV-COOH) were obtained from Lifetein (NJ). PureYield Plasmid Miniprep kit, Wizard SV Gel and PCR Clean-Up system, furimazine substrate, and pNL1.1 were obtained from Promega (WI). All other chemicals and reagents used were from Fujifilm Wako Pure Chemicals (Osaka, Japan).

Plasmid Constructions. To construct the expression vectors for Nluc−scFv and scFv−Nluc, the fragment encoding Nluc was amplified via PCR using the two sets of primers, NlucNdeBack and NlucNdeFor, or NlucBamBack and NlucBamFor, using pNL1.1 as a template. The sequences of the primers used in this study are summarized in the Supporting Information Table S1. The amplified fragment was inserted to the unique *Nde*I or *Bam*HI site of pSQ(KTM219), respectively, which is the plasmid encoding a Cys-tagged anti-BGP scFv,[17] using an In-Fusion HD Cloning Kit (Takara-bio, Shiga, Japan), to yield pNL-SQ(KTM219) and pSQ(KTM219)NL, respectively. The mixed base (W) in the forward primers allowed yielding expression vectors for Nluc(C166S)−scFv and scFv−Nluc(C166S), harboring C166S mutation in Nluc. To construct the expression vector for Nluc_G_3S-scFv, the fragment encoding Nluc_G_3S was amplified via PCR using the primers, NlucNdeBack and G3SNlucNdeFor, digested with *Nde*I, and inserted to the *Nde*I site of pNL-SQ(KTM219) by dephosphorylation and ligation. To obtain the expression vector for Nluc_d4-scFv, a shorter Nluc fragment was amplified with primers NlucNdeBack and Nlucd4AgeFor, digested with *Nde*I and *Age*I, and inserted between the same sites in pNL-SQ(KTM219).

Protein Expressions and Purification. The proteins were expressed in *Escherichia coli* SHuffle T7 Express lysY in 200 mL of the medium and purified using TALON metal affinity resin, as described previously.[24] More details are described in the "Materials and Methods" section in the SI.

Fluorescence Labeling. The purified proteins (0.5 nmol) were labeled with maleimide dye to prepare BRET Q-bodies. To this end, the exposed thiol group in Cys tag was reduced in 100 μL of 10 mM phosphate-buffered saline (PBS), pH 6.1, containing 0.05% Tween20, 2.5 mM tris(2-carboxyethyl)-phosphine hydrochloride (TCEP), and 10 mM Ethylenediaminetetraacetic acid for 30 min at 25 °C, and the TCEP was quenched by adding 10 mM 4-azidobenzoic acid for 10 min at pH 6.0 as described previously.[37] Afterward, the maleimide dye (0.5 μL of 10 mM TAMRA-C5-mal, 10 mM ATTO520-C2-mal, or 5 mM R6G-C2-mal, each in dimethylsulfoxide) was added to the solution and labeled in the dark for 1 h at 25 °C and for 16 h at 4 °C. The molar ratio of the protein to the dye was set to 1:10. To remove the free dye, the BRET Q-body was purified via the FLAG M2 Affinity Gel (Sigma-Aldrich), as indicated by the manufacturer, except that 400 μL of PBS containing 0.1% poly(oxethylene) lauryl ether (Brij 35) was used for washing five times. The proteins were eluted with 150 μg/mL 3xFLAG peptide in PBS 0.1% Brij 35. Sodium dodecyl sulfate-polyacrylamide gel electrophoresis (SDS-PAGE) was performed using a 12.5% polyacrylamide gel. The sample was either boiled for 90 s in the sample buffer including 10 mM dithiothreitol (DTT) or not boiled in the sample buffer without DTT before application.

Fluorescence and Bioluminescence Measurements. The irradiation-based and BRET-based luminescent spectra of 40 nM each of the BRET Q-body in 250 μL of PBS containing 0.05% Tween20 and 0.1% bovine serum albumin, pH 7.4 (PBSTB), were determined in a quartz microcuvette (5 mm × 5 mm) using an FP-8500 spectrofluorometer (Jasco, Tokyo, Japan) equipped with a rotating sample changer and a magnetic stirrer at 25 °C. Increasing concentrations of the antigen BGP-C7 in PBSTB were added in titration in constant (∼5 min) intervals. As a control, the same volume of PBSTB was added to a reference cuvette for correcting the time-dependent attenuation of the signal during the titration due to the increased volume, photobleaching, or substrate consumption.

https://doi.org/10.1021/acs.analchem.0c05217
Anal. Chem. 2021, 93, 7571−7578

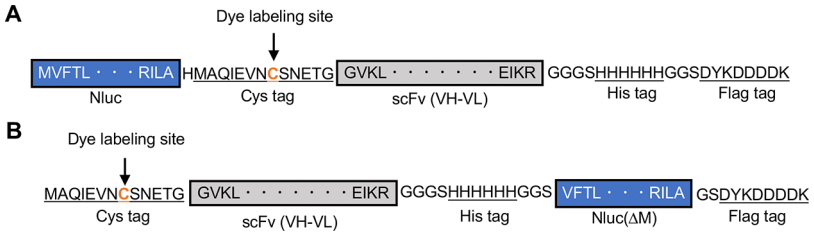

Figure 2. Amino-acid sequences of the fusion proteins around Nluc and scFv. The Cys residues used for dye labeling are also shown. Nluc was either fused to the N-terminal (A) or to the C-terminal (B) side of scFv. His and Flag tags are used for tandem purification before and after dye labeling.

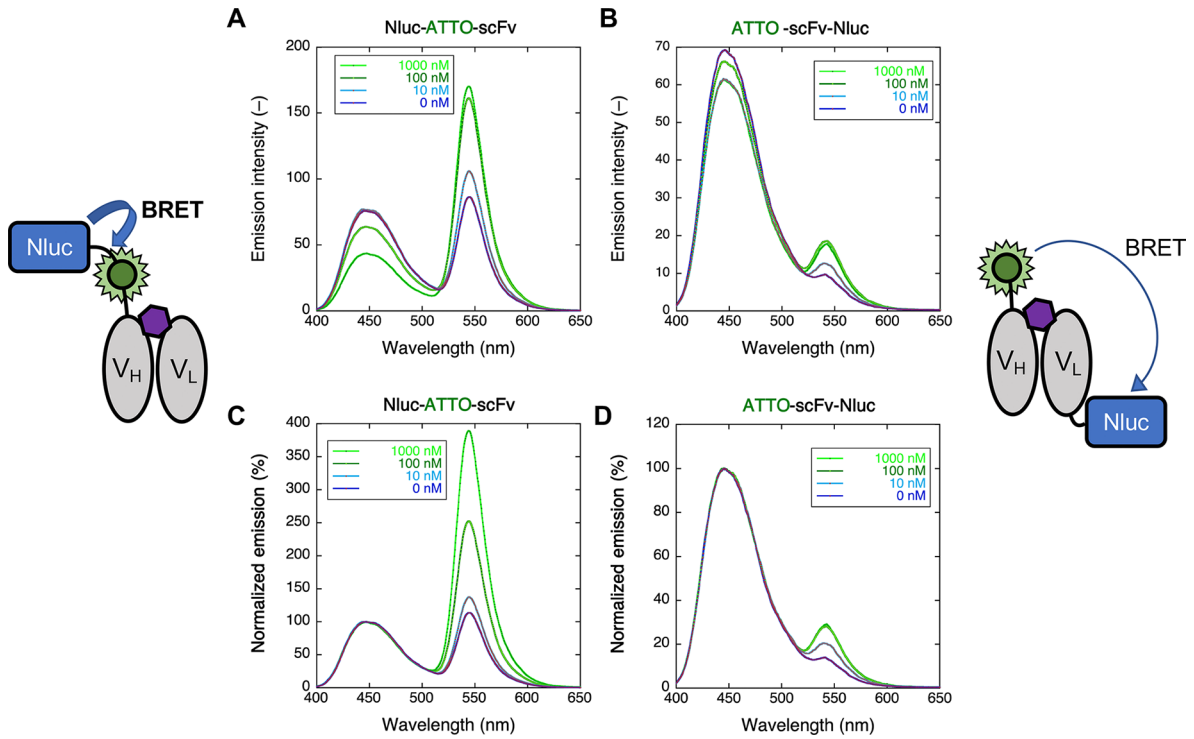

Figure 3. Effect of Nluc fusion position. The emission spectra in the presence of an indicated concentration of antigen BGP-C7 from the N-terminal (A, C) and the C-terminal (B, D) fusion proteins are shown as raw (A, B) and normalized (C, D) spectra. Proteins used: 40 nM.

$$E_{\mathrm{correct}}(t) = E_{\mathrm{antigen}}(t) \cdot \frac{E_{\mathrm{maxPBSTB}}(t_0)}{E_{\mathrm{maxPBSTB}}(t)} \quad (1)$$

where $E_{\mathrm{correct}}(t)$ and $E_{\mathrm{antigen}}(t)$ are the corrected and actual emission intensities of the antigen-added sample, respectively, and $E_{\mathrm{maxPBSTB}}(t_0)$ and $E_{\mathrm{maxPBSTB}}(t)$ are the maximum emission intensities of the buffer-added sample at time t_0 and t, respectively. For the irradiation-based assay, excitations at 524/5, 546/5, and 528/5 nm for ATTO520-, tetramethylrhodamine (TAMRA)-, and rhodamine 6G (R6G)-labeled BRET Q-body were used, respectively. BRET-based luminescent emission spectra were measured in the presence of furimazine (1/200 in v/v) without irradiation of the excitation light.

To determine the dose response, triplicate samples were measured using a microplate-based spectrophotometer ClarioStar (BMG Labtech Japan, Saitama, Japan) at their peak wavelength(s) without correction. For the irradiation-based assays, a 1 nM BRET Q-body with varied concentrations of the antigen in 100 μL of PBSTB was applied to a black half-well 96-well plate, incubated at 25 °C for 20 min, and then the fluorescence intensity was measured with excitations at 500/28, 520/28, and 540/28 nm for ATTO520-, TAMRA-, and R6G-labeled BRET Q-body, respectively. For the BRET-based assay, the 1 nM BRET Q-body with varied concentrations of the antigen in 100 μL PBSTB was applied to a white half-well 96-well plate, incubated at 25 °C for 20 min, and furimazine substrate (1/33 in 20 μL PBSTB) was added just before the measurement. Dose−response curves were fitted to a four-parameter logistic equation using ImageJ software (http://rsbweb.nih.gov/ij/). The EC_{50} and limit of detection (LOD) were calculated as the concentration corresponding to the mean blank value plus 3 times the standard deviation (SD) for each assay.

Bioluminescence Observation. For observing and taking images of bioluminescence, 10 nM BRET Q-body with and without 2 μM BGP-C7 in 50 μL of PBS containing 0.05% Tween20, pH 7.4 (PBST), placed in a 96-well white microplate was added with a 1/100 (v/v) furimazine substrate in 50 μL of PBST in a dark room, and a picture was taken with a digital camera α7S (Sony, Tokyo, Japan) at ISO8000, F1/2, exposed for 5 s.

https://doi.org/10.1021/acs.analchem.0c05217
Anal. Chem. 2021, 93, 7571−7578

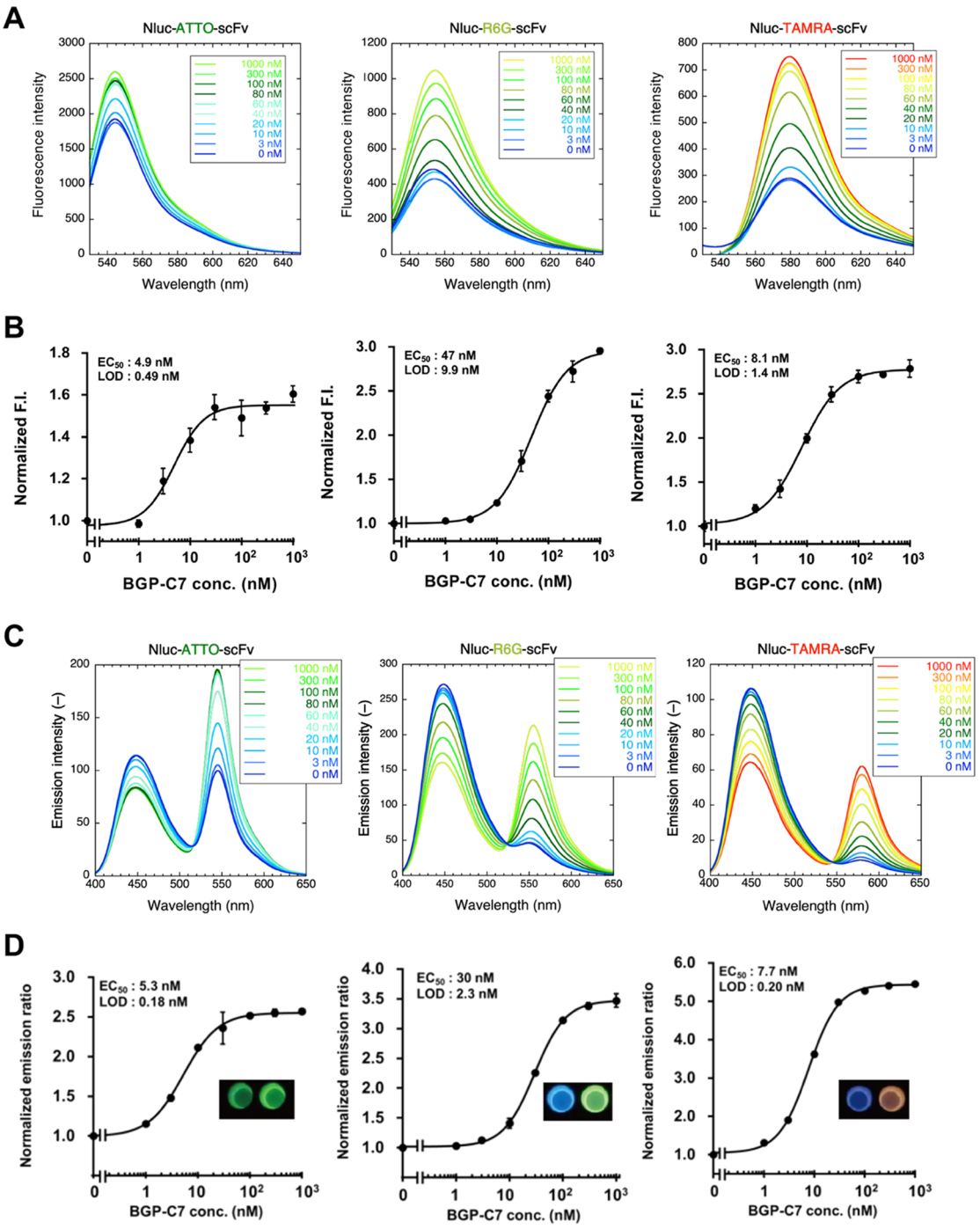

Figure 4. Irradiation-based (A, B) and BRET-based (C, D) luminescent responses of the BRET Q-bodies labeled with ATT520, R6G, and TAMRA. Luminescent spectra (A, C) were recorded with 40 nM proteins, together with the same reaction mixture without adding antigen BGP-C7 to correct time-dependent luminescence decay. The dose responses (B, D) were measured using a microplate reader at the same protein concentration (1 nM). Averages ± 1 SD are shown. The insets in (D) show the color images for the BRET-based luminescence from the 10 nM BRET Q-body with and without 2 μM BGP-C7.

RESULTS AND DISCUSSION

In this study, BGP-C7, a C-terminal peptide (seven aa) of the bone metabolism marker osteocalcin/BGP, was used as a target antigen. Recently, BGP has also attracted attention for its unprecedented functions in glucose homeostasis,[38] brain development,[39] and male fertility.[40] The BRET Q-body was prepared using an anti-BGP scFv. Upon preparation, there was a concern that Nluc might inhibit dye labeling or antigen binding if Nluc and the dye-labeling site are too close to each other. On the other hand, Nluc and the dye needed to be close enough to allow efficient energy transfer. Therefore, we prepared two fusion variants, i.e., one in which Nluc was fused to the scFv N-terminus (Nluc−scFv) and the other in which Nluc was fused to the scFv C-terminus (scFv−Nluc); a dye was then introduced to a cysteine (Cys) residue in a flexible linker (Cys tag, MAQIEVNCSNETG) at the N-terminal of scFv using the maleimide−thiol reaction (Figure

https://doi.org/10.1021/acs.analchem.0c05217
Anal. Chem. 2021, 93, 7571−7578

2). Therefore, we prepared two fusion proteins of Nluc−scFv and scFv−Nluc.

Before the dye-labeling reaction, we investigated whether the Nluc−scFv/scFv−Nluc fusion proteins retained the antigen-binding activity using antigen-immobilized enzyme-linked immunosorbent assay (ELISA) (Supporting Information, Figure S1). For both probes, signals in antigen (biotinylated BGP-C11)-immobilized wells were substantially greater than those in wells without the antigen, indicating that the fusion proteins retained the specific antigen-binding activity. The lower signals for scFv−Nluc might be due to the lower accessibility of His_6 tag between scFv and Nluc. Next, we labeled the two Nluc−scFv/scFv−Nluc fusion proteins with ATTO520-C2-maleimide, a dye known to be suitable for making Q-bodies. We chose ATTO520 also because its excitation spectrum has a sufficiently large overlap with the emission spectrum of Nluc, which is one of the prerequisites to select a suitable dye for BRET. After the labeling reaction, we removed free dye molecules by extensive purification using an antibody against the Flag tag that was appended to the C-terminus of fusion proteins (SI Figure S2).

First, emission spectra of the two ATTO520-labeled probes were measured in the presence of the substrate furimazine without irradiation with excitation light (Figure 3). The performance of the BRET Q-body was evaluated from the two viewpoints of antigen-dependent response and BRET efficiency. Consequently, the emission intensity of the dye-derived peak increased upon antigen addition, and the observed maximum increase for Nluc−ATTO−scFv and ATTO−scFv−Nluc was 2.0- and 1.9-fold, respectively (Figure 3A,B). Since the maximum luminescence ratios of the dye-derived peak per Nluc-derived peak for Nluc−ATTO−scFv and ATTO−scFv−Nluc were 3.4- and 2.1-fold, respectively (Figure 3C,D), the observed BRET efficiency was higher for Nluc−scFv, probably reflecting a shorter Nluc dye distance. Next, we focused on the solvent-semiexposed Cys166 in Nluc that can potentially affect the folding of fusion proteins or promiscuous labeling of the maleimide dye or both. To evaluate these possibilities, we also prepared the same pair with a mutant Nluc that had a mutation of C166S. When we tested the fusion proteins with this mutation, it was observed that there were no positive effects on the responses, especially for Nluc(C166S)−ATTO520−scFv that showed lower antigen dependency and BRET efficiency (SI Figures S1−S3). Hence, we decided to use the wild-type (WT) Nluc−scFv fusion protein for further analyses.

Next, we compared the antigen dependency of irradiation-based and BRET-based emission spectra of Nluc−scFvs, which were labeled with R6G or TAMRA in addition to ATTO520. To compensate changes in the Nluc-derived emission intensity by the increase in the sample volumes, photobleaching, and substrate consumption, emission intensities of samples containing the same volume of the buffer instead of the antigen solution were simultaneously measured as a control. First, fluorescence spectra of dye-labeled fusion proteins were measured using appropriate excitation light in the absence of the luminescent substrate. The fluorescence intensity increased depending on the antigen concentration; the observed maximum increase in the fluorescence intensity for ATTO-, R6G-, and TAMRA-labeled BRET Q-bodies was 1.3-, 2.2-, and 2.6-fold, respectively (Figure 4A).

Next, emission spectra of these BRET Q-bodies without excitation light in the presence of the substrate furimazine were measured, demonstrating that the emission peak intensity increased upon antigen addition by up to 1.9-, 4.8-, and 7.2-fold for ATTO-, R6G-, and TAMRA-labeled BRET Q-bodies, respectively (Figure 4C).

Although we expected similar BRET-based luminescent responses, surprisingly, for all of the BRET Q-bodies, higher luminescent responses were obtained for BRET-based assays than the irradiation-based ones as conventional Q-bodies.

Furthermore, the maximum emission intensity ratios of dye-/Nluc-derived peaks observed for ATTO-, R6G-, and TAMRA-labeled BRET Q-bodies were 2.7-, 7.9-, and 12-fold, respectively, which showed even higher values. This was owing to an antigen-dependent decrease of Nluc-derived emission, which means an antigen-dependent increase in BRET efficiency, probably reflecting antigen-dependent approximation of the dye to Nluc.

When the dose−response curves were drawn with three samples using a 96-well plate reader at the same BRET Q-body concentration, higher responses of the luminescence-based ratiometric measurement were also observed (Figure 4BD). Because of the smaller errors due to ratiometric measurement, lower limits of detection were consistently observed for all of the BRET Q-bodies. Moreover, Nluc-derived luminescence can be observed in the dark using a digital camera for at least several minutes because of its stability and intensity. Upon addition of the antigen, a shift from the initial cyan color to a color close to the fluorescence of the dye used for labeling was observed (see the inset in Figure 4D). This result demonstrates that the BRET Q-body system can be used to visualize the presence or the absence of an antigen as a change in the emission color without any instrument. Among the three BRET Q-bodies, Nluc−TAMRA−scFv, which showed the highest antigen-dependent response and spectral change, was considered to be used as the best BRET Q-body.

As a possible reason why BRET-based responses were greater than the irradiation-based assay using the same BRET Q-bodies, we speculated the contamination of nonfunctional protein during the BRET Q-body preparation. The nonfunctional BRET Q-bodies cannot bind to the antigen but are labeled with the dye, increasing the background signal and reducing antigen responses when excited; meanwhile, inappropriately folded BRET Q-bodies do not produce light emission, and thus do not reduce antigen responses in BRET.

To examine this possibility, BRET Q-bodies were analyzed by less-denaturing electrophoresis (SI Figure S5). The BRET Q-bodies were subjected to SDS-PAGE, either after denaturation by heating in the presence of DTT or without the denaturation treatment. In the following SDS-PAGE, the nondenatured protein, which is supposed to be correctly folded, migrates faster and is thus detected as a band at a lower position than a denatured one with the same molecular weight. On the other hand, even without the denaturing treatment, an inappropriately folded protein is likely to be detected as a band at the same (or near) position as that of the denatured protein. As a result, although TAMRA-labeled Nluc−scFv without the denaturation treatment showed slightly split two bands, other Nluc−scFv proteins without the denaturation treatment only showed bands at lower positions and thus could not be confirmed to contain inappropriately folded proteins.

From this result, we reasoned that the dye movement induces the antigen-dependent increase of BRET efficiency: upon antigen binding, the dye and Nluc are brought closer, and thus the BRET reaction is facilitated. To better understand

https://doi.org/10.1021/acs.analchem.0c05217
Anal. Chem. 2021, 93, 7571−7578

the mechanism of antigen-dependent BRET efficiency increase, BRET Q-bodies with different lengths of the linker between Nluc and the dye were prepared. BRET Q-body constructs with a four residue (GGGS) longer linker sequence (Nluc_G_3S-scFv) and a four residue shorter linker sequence (Nluc_d4-scFv) were made, and TAMRA-labeled proteins were prepared as before (Figure 5A). Also, TAMRA-labeled

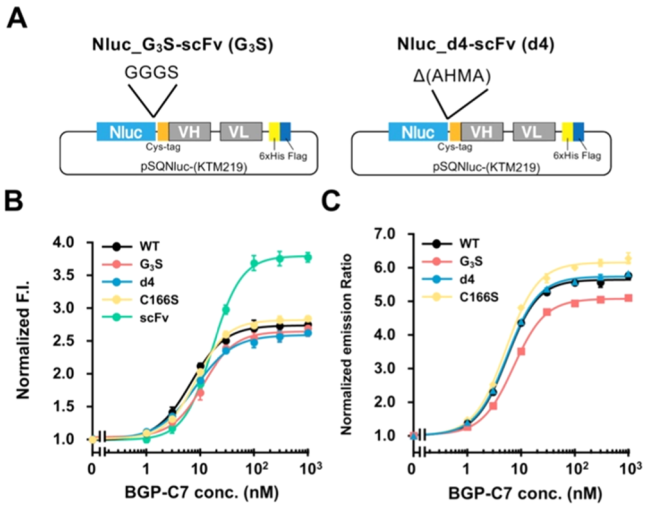

Figure 5. Effects of the linker length between Nluc and the TAMRA fluorescent dye and Nluc C166S mutation. (A) Schematic structure of the linker mutants. (B, C) Dose responses of (B) irradiation-based and (C) BRET-based luminescence of the wild type (WT), Nluc_G_3S-scFv (G3S), Nluc_d4-scFv (d4), Nluc(C166S)-scFv (C166S), and scFv (only for B). Averages ±1 SD are shown. Protein concentration: 1 nM.

Nluc(C166S)-scFv was prepared to compare the response (SI Figures S6 and S7). To ensure that these modifications did not affect the dye-labeling reaction and the folding of the scFv moiety, the fluorescent dye/protein (F/P) ratios and antigen-binding activity were determined from the absorption spectra and biolayer interferometry (BLI), respectively. As a result, the calculated F/P ratios were similar (between 1 and 1.2) for all of the variants including TAMRA-labeled Nluc(C166S)-scFv and the scFv Q-body without Nluc (SI, Table S2, Figures S8 and S9), and their antigen-binding activity confirmed to be almost the same (SI Table S3 and Figure S10).

It is worth noting that although a quenching dimer (H dimer)-derived absorption peak at 520 nm[41] was observed for all of the absorption spectra including that of scFv without Nluc, it mostly disappeared when an excess amount of the antigen BGP-C7 was added (SI, Figure S9). This unprecedented phenomenon of enhanced H dimer formation in the absence of an antigen might be explained by the dimerization of two dyes in the interior of dimerized scFv (diabody[42]), which results in the enhanced quenching of not only BRET Q-bodies but also normal Q-bodies. Although a detailed analysis of this phenomenon awaits future investigation, it is unlikely that the observed H dimer peak is due to the labeling of the sensor proteins at the other site than Cys in the Cys tag. The somewhat higher *F/P* ratios observed might reflect the remaining free dye after purification.

Next, the irradiation-based and BRET-based dose responses were determined using a microplate reader as before (Figure 5 BC and SI, Table S4). As expected, the variants with a longer and a shorter linker and Nluc(C166S)-scFv showed similar irradiation-based responses to the original TAMRA-labeled Nluc−scFv. In contrast, the longer linker variant Nluc_G_3S-scFv showed slightly lower responses, probably reflecting a decreased BRET efficiency change. It is worth noting that although the maximum irradiation-based responses of BRET Q-bodies were less than that of the scFv Q-body without Nluc, their BRET-based responses were consistently higher. The lower irradiation-based responses of BRET Q-bodies might be due to the quenching by tethered Nluc with three Trp residues. Further investigation is expected to clarify this issue in future. In conclusion, the linker length and Nluc C166S mutation on the antigen response of BRET Q-bodies were not critically important, suggesting the robustness of the BRET Q-body approach.

CONCLUSIONS

In the present study, we succeeded in the development of a BRET Q-body, which shows higher antigen dependency in intensity ratios than that in the fluorescent intensity change of the original Q-body. Compared with the conventional Q-body, the measurement based on ratiometric detection is enhanced by antigen-dependent BRET and is more accurate because it is less sensitive to the amount of the probe. Also, it is neither necessary to use an external excitation light source nor consider photobleaching by strong excitation light. BRET-based biosensors are considered useful as a core of the point-of-care test, and those based on Nluc for detecting an antibody and an antigen are reported.[34−36] Compared with reported systems, our BRET Q-body system is based on the novel detection principle: quenching of the fluorescent dye and its antigen-dependent dequenching. It has the potential to convert already developed Q-bodies to a bioluminescent sensor with higher sensitivity and enhanced response. Also, the detection of the BRET signal does not need a light source, allows visual observation of the color change, and easier integration to a smartphone-based device. Therefore, we expect that BRET Q-bodies will be a promising tool for diagnosis, food safety, environmental preservation, and biological research.

ASSOCIATED CONTENT

Supporting Information

The Supporting Information is available free of charge at https://pubs.acs.org/doi/10.1021/acs.analchem.0c05217.

(Tables S1−4) Oligonucleotides used, F/P ratios, kinetic constants, and the luminescent responses of the TAMRA-labeled Q-bodies; (Figures S1−S10) antigen-binding ELISA, SDS-PAGE analysis of BRET Q-bodies, bioluminescence response of Nluc(C166S) BRET Q-bodies, BLI sensorgrams, the structure of linker mutants, and characterization of TAMRA-labeled mutants by absorption spectroscopy and biolayer interferometry (PDF)

AUTHOR INFORMATION

Corresponding Author

Hiroshi Ueda − *Laboratory for Chemistry and Life Science, Institute of Innovative Research, Tokyo Institute of Technology, Yokohama, Kanagawa 226-8503, Japan;* orcid.org/0000-0001-8849-4217; Email: ueda@res.titech.ac.jp

https://doi.org/10.1021/acs.analchem.0c05217
Anal. Chem. 2021, 93, 7571−7578

Authors

Riho Takahashi − *Graduate School of Life Science and Technology, Tokyo Institute of Technology, Yokohama, Kanagawa 226-8503, Japan*

Takanobu Yasuda − *Graduate School of Life Science and Technology, Tokyo Institute of Technology, Yokohama, Kanagawa 226-8503, Japan*

Yuki Ohmuro-Matsuyama − *Laboratory for Chemistry and Life Science, Institute of Innovative Research, Tokyo Institute of Technology, Yokohama, Kanagawa 226-8503, Japan;* Present Address: Technology Research Laboratory, Shimadzu Co. Ltd., Hikaridai, Seika-cho, Soraku-gun, Kyoto 619-0237, Japan

Complete contact information is available at: https://pubs.acs.org/10.1021/acs.analchem.0c05217

Author Contributions

R.T. and T.Y. contributed equally; H.U. designed experiments; R.T. and T.Y. performed all experiments; and Y.O.-M. and H.U. wrote the manuscript. All authors have approved the final version of the manuscript.

Funding

This work was supported in part by JSPS KAKENHI Grant Numbers JP18H03851 (to H.U.) and JP17K06920 (to Y.O.M.), from the Japan Society for the Promotion of Science, Japan, and the JST-Mirai Program Grant Number JPMJMI18D9 from Japan Science and Technology Agency, Japan.

Notes

The authors declare no competing financial interest.

■ ACKNOWLEDGMENTS

The authors acknowledge Tetsuya Kitaguchi, Hiroyuki Nakamura, and Kazuki Miura for valuable advice, the Biomaterials Analysis Division, Open Facility Center, Tokyo Institute of Technology for DNA sequence analysis, and the support by the Dynamic Alliance for Open Innovation Bridging Human, Environment and Materials from MEXT, Japan.

■ REFERENCES

(1) Balamurugan, M.; Santharaman, P.; Madasamy, T.; Rajesh, S.; Sethy, N. K.; Bhargava, K.; Kotamraju, S.; Karunakaran, C. *Biosens. Bioelectron.* **2018**, *116*, 89−99.

(2) DeLaney, K.; Buchberger, A. R.; Atkinson, L.; Grunder, S.; Mousley, A.; Li, L. *J. Exp. Biol.* **2018**, *221*, No. jeb151167.

(3) Kabe, Y.; Sakamoto, S.; Hatakeyama, M.; Yamaguchi, Y.; Suematsu, M.; Itonaga, M.; Handa, H. *Anal. Bioanal. Chem.* **2019**, *411*, 1825−1837.

(4) Zhang, Y.; Luo, J.; Flewitt, A. J.; Cai, Z.; Zhao, X. *Biosens. Bioelectron.* **2018**, *116*, 1−15.

(5) Balahura, L. R.; Stefan-Van Staden, R. I.; Van Staden, J. F.; Aboul-Enein, H. Y. *J. Immunoassay Immunochem.* **2019**, *40*, 40−51.

(6) Saraswati, K.; Phanichkrivalkosil, M.; Day, N. P. J.; Blacksell, S. D. *PLoS Neglected Trop. Dis.* **2019**, *13*, No. e0007158.

(7) Hörber, S.; Achenbach, P.; Schleicher, E.; Peter, A. *Biotechnol. Adv.* **2020**, *39*, No. 107359.

(8) Engin, E. D. *J. Immunoassay Immunochem.* **2019**, *40*, 109−122.

(9) Rahman, H. U.; Yue, X.; Yu, Q.; Xie, H.; Zhang, W.; Zhang, Q.; Li, P. *J. Sci. Food Agric.* **2019**, *99*, 4869−4877.

(10) Do, A. B.; Khuda, S. E.; Sharma, G. M. *J. AOAC Int.* **2018**, *101*, 23−35.

(11) Chen, W.; Huang, Z.; Hu, S.; Peng, J.; Liu, D.; Xiong, Y.; Xu, H.; Wei, H.; Lai, W. *J. Dairy Sci.* **2019**, *102*, 1887−1900.

(12) Daniels, T.; Earlywine, M.; Breeding, V. *Am. J. Infect. Control* **2019**, *47*, 400−405.

(13) Behera, B. K.; Das, A.; Sarkar, D. J.; Weerathunge, P.; Parida, P. K.; Das, B. K.; Thavamani, P.; Ramanathan, R.; Bansal, V. *Environ. Pollut.* **2018**, *241*, 212−233.

(14) Fang, T. Y.; Praveena, S. M.; deBurbure, C.; Aris, A. Z.; Ismail, S. N. S.; Rasdi, I. *Chemosphere* **2016**, *165*, 358−368.

(15) Abe, R.; Ohashi, H.; Iijima, I.; Ihara, M.; Takagi, H.; Hohsaka, T.; Ueda, H. *J. Am. Chem. Soc.* **2011**, *133*, 17386−17394.

(16) Abe, R.; Jeong, H. J.; Arakawa, D.; Dong, J. H.; Ohashi, H.; Kaigome, R.; Saiki, F.; Yamane, K.; Takagi, H.; Ueda, H. *Sci. Rep.* **2014**, No. 4640.

(17) Jeong, H.-J.; Kawamura, T.; Dong, J.; Ueda, H. *ACS Sens.* **2016**, *1*, 88−94.

(18) Dong, J.; Ueda, H. *Sensors* **2021**, *21*, No. 1223.

(19) Jeong, H. J.; Ohmuro-Matsuyama, Y.; Ohashi, H.; Ohsawa, F.; Tatsu, Y.; Inagaki, M.; Ueda, H. *Biosens. Bioelectron.* **2013**, *40*, 17−23.

(20) Jeong, H. J.; Ueda, H. *Sensors* **2014**, *14*, 13285−13297.

(21) Ohashi, H.; Matsumoto, T.; Jeong, H. J.; Dong, J. H.; Abe, R.; Ueda, H. *Bioconjugate Chem.* **2016**, *27*, 2248−2253.

(22) Jeong, H. J.; Matsumoto, K.; Itayama, S.; Kodama, K.; Abe, R.; Dong, J. H.; Shindob, M.; Ueda, H. *Chem. Commun.* **2017**, *53*, 10200−10203.

(23) Zhao, S. T.; Dong, J. H.; Jeong, H. J.; Okumura, K.; Ueda, H. *Anal. Bioanal. Chem.* **2018**, *410*, 4219−4226.

(24) Jeong, H. J.; Dong, J. H.; Ueda, H. *Sensors* **2019**, *19*, No. 52.

(25) Hall, M. P.; Unch, J.; Binkowski, B. F.; Valley, M. P.; Butler, B. L.; Wood, M. G.; Otto, P.; Zimmerman, K.; Vidugiris, G.; Machleidt, T.; Robers, M. B.; Benink, H. A.; Eggers, C. T.; Slater, M. R.; Meisenheimer, P. L.; Klaubert, D. H.; Fan, F.; Encell, L. P.; Wood, K. V. *ACS. Chem. Biol.* **2012**, *7*, 1848−1857.

(26) England, C. G.; Ehlerding, E. B.; Cai, W. B. *Bioconjugate Chem.* **2016**, *27*, 1175−1187.

(27) Mo, X. L.; Fu, H. A. BRET: NanoLuc-Based Bioluminescence Resonance Energy Transfer Platform to Monitor Protein-Protein Interactions in Live Cells. In *High Throughput Screening: Methods and Protocols*, 3rd ed.; Humana Press: New York, NY, 2016; Vol. *1439*, pp 263−271.

(28) Dimri, S.; Basu, S.; De, A. Use of BRET to Study Protein-Protein Interactions In Vitro and In Vivo. In *Nuclear Receptor Superfamily: Methods and Protocols*; 2nd ed.; Humana Press: New York, NY, 2016; Vol. *1443*, pp 57−78.

(29) Dale, N. C.; Johnstone, E. K. M.; White, C. W.; Pfleger, K. D. G. *Front. Bioeng. Biotechnol.* **2019**, *7*, No. 56.

(30) White, C. W.; Johnstone, E. K. M.; See, H. B.; Pfleger, K. D. G. *Cell. Signalling* **2019**, *54*, 27−34.

(31) Pernomian, L.; Gomes, M. S.; Moreira, J. D.; da Silva, C. H. T. D.; Rosa, J. M. C.; Cardoso, C. R. D. *Curr. Radiopharm.* **2017**, *10*, 16−20.

(32) Stoddart, L. A.; Kilpatrick, L. E.; Hill, S. J. *Trends Pharmacol. Sci.* **2018**, *39*, 136−147.

(33) Machleidt, T.; Woodroofe, C. C.; Schwinn, M. K.; Mendez, J.; Robers, M. B.; Zimmerman, K.; Otto, P.; Daniels, D. L.; Kirkland, T. A.; Wood, K. V. *ACS Chem. Biol.* **2015**, *10*, 1797−1804.

(34) Arts, R.; den Hartog, I.; Zijlema, S. E.; Thijssen, V.; van der Beelen, S. H.; Merkx, M. *Anal. Chem.* **2016**, *88*, 4525−4532.

(35) van Rosmalen, M.; Ni, Y.; Vervoort, D. F. M.; Arts, R.; Ludwig, S. K. J.; Merkx, M. *Anal. Chem.* **2018**, *90*, 3592−3599.

(36) Xue, L.; Yu, Q. L. Y.; Griss, R.; Schena, A.; Johnsson, K. *Angew. Chem., Int. Ed.* **2017**, *56*, 7112−7116.

(37) Henkel, M.; Rockendorf, N.; Frey, A. *Bioconjugate Chem.* **2016**, *27*, 2260−2265.

(38) Lee, N. K.; Sowa, H.; Hinoi, E.; Ferron, M.; Ahn, J. D.; Confavreux, C.; Dacquin, R.; Mee, P. J.; McKee, M. D.; Jung, D. Y.; Zhang, Z.; Kim, J. K.; Mauvais-Jarvis, F.; Ducy, P.; Karsenty, G. *Cell* **2007**, *130*, 456−469.

(39) Oury, F.; Khrimian, L.; Denny, C. A.; Gardin, A.; Chamouni, A.; Goeden, N.; Huang, Y. Y.; Lee, H.; Srinivas, P.; Gao, X. B.;

Suyama, S.; Langer, T.; Mann, J. J.; Horvath, T. L.; Bonnin, A.; Karsenty, G. *Cell* **2013**, *155*, 228−241.
(40) Oury, F.; Sumara, G.; Sumara, O.; Ferron, M.; Chang, H.; Smith, C. E.; Hermo, L.; Suarez, S.; Roth, B. L.; Ducy, P.; Karsenty, G. *Cell* **2011**, *144*, 796−809.
(41) Christie, R. J.; Tadiello, C. J.; Chamberlain, L. M.; Grainger, D. W. *Bioconjugate Chem.* **2009**, *20*, 476−480.
(42) Holliger, P.; Prospero, T.; Winter, G. *Proc. Natl. Acad. Sci. U.S.A.* **1993**, *90*, 6444−6448.

https://doi.org/10.1021/acs.analchem.0c05217
Anal. Chem. 2021, 93, 7571−7578